

Crystallization of the pectate lyase PelI from *Erwinia chrysanthemi* and SAD phasing of a gold derivative

Sandra Castang,^a Vladimir E. Shevchik,^a Nicole Hugouvieux-Cotte-Pattat,^a Pierre Legrand,^{b†} Richard Haser^c and Patrice Gouet^{c*}

^aComposante INSA de l'Unité de Microbiologie et Génétique, UMR 5122 CNRS-UCBL-INSA, Bâtiment A. Lwoff, 10 Rue R. Dubois, 69622 Villeurbanne, France, ^bInstitut de Biologie Structurale, UMR 5075 CNRS-CEA-UJF, 41 Rue Jules Horowitz, 38027 Grenoble CEDEX 1, France, and ^cLaboratoire de BioCristallographie, Institut de Biologie et Chimie des Protéines, UMR 5086 CNRS-UCBL, 7 Passage du Vercors, 69367 Lyon, France

† Present address: EMBL Grenoble, 6 Rue Jules Horowitz, BP 181, 38042 Grenoble CEDEX 9, France.

Correspondence e-mail: p.gouet@ibcp.fr

The pectate lyase PelI is involved in the degradation of plant tissues by the phytopathogenic bacterium *Erwinia chrysanthemi*. It has been crystallized from a solution containing PEG 550 in the space group $P2_1$, with unit-cell parameters $a = 61.6$, $b = 70.7$, $c = 73.4$ Å, $\beta = 112.8^\circ$. Crystals diffract to 1.45 Å using synchrotron radiation. SAD phases have been computed from a gold-derivative crystal at the wavelength of maximum absorption (L_{III} edge).

Received 29 September 2003

Accepted 13 November 2003

1. Introduction

The enterobacterium *Erwinia chrysanthemi* is a causative agent of soft-rot disease in a wide variety of plants. Among a set of pectin-depolymerizing enzymes produced by *Erwinia*, the pectate lyases (Pel) are the major pectinases and play a key role in plant-tissue maceration (Robert-Baudouy *et al.*, 2000). These enzymes catalyse the cleavage of pectate (homogalacturonan) by β -elimination, breaking the α -glycosidic bond between O₁ and C₄ to leave an unsaturated C₄–C₅ bond. This mechanism is metal-ion-dependent: Ca²⁺ is the cofactor of most known Pels, while Co²⁺, Cu²⁺, Mn²⁺ or Ni²⁺ are required by some intracellular Pels involved in degradation of pectic oligomers (Shevchik *et al.*, 1999). By sequence analysis, Pels are classed into five distinct families, numbered 1, 2, 3, 9 and 10, of the 13 families of polysaccharide lyases classified in the CAZy database (Coutinho & Henrissat, 1999). The Pels produced by *E. chrysanthemi* are members of families 1 (PelA–PelE and PelZ), 2 (PelW), 3 (PelI) and 9 (PelL and PelX).

The three-dimensional structures of several Pels from families 1, 3 and 10 have been determined (Yoder *et al.*, 1993; Leitzke *et al.*, 1994; Pickersgill *et al.*, 1994; Akita *et al.*, 2001; Charnock *et al.*, 2002; Thomas *et al.*, 2002; Herron *et al.*, 2003). Most of these proteins have a right-handed parallel β -helix fold (Jurnak *et al.*, 1994). This protein fold, which was first reported for *E. chrysanthemi* PelC (Yoder *et al.*, 1993), is shared with many polysaccharide-active enzymes, mostly pectinases (Mayans *et al.*, 1997; Petersen *et al.*, 1997; Pickersgill *et al.*, 1998; Vitali *et al.*, 1998; Jenkins *et al.*, 2001). It is also shared with polysaccharide lyases of families 1, 3 and 9, carbohydrate esterases of family 8 and glycoside hydrolases of family 28 (CAZy). Thus, it was speculated that the β -helix fold could be particularly adapted to polysaccharide binding.

However, a new polysaccharide lyase fold with an $(\alpha/\alpha)_3$ barrel has been described in a recent report (Charnock *et al.*, 2002).

The pectate lyase PelI belongs to family 3 and is the only known example from the *E. chrysanthemi* pectinases that consists of two functional modules, named the N-terminal and catalytic domains. These two domains are separated in external media by a specific cleavage produced by *E. chrysanthemi* proteases (Shevchik *et al.*, 1998). The catalytic domain of PelI released by proteolysis seems to possess the same enzymatic properties *in vitro* as the full-length protein. However, contrarily to the full-length PelI, the catalytic domain elicits a necrotic reaction *in planta* associated with an active defence by plants. This type of reaction, called a hypersensitive response (HR), is unusual for Pels, but is characteristic of a set of effector proteins secreted by the type III secretion systems of many plant pathogenic bacteria (Buttner & Bonas, 2003). It should be noted that family 3 of polysaccharide lyases also includes HrpW, the HR elicitor protein without pectate lyase activity, secreted by the type III secretion system (Gaudriault *et al.*, 1998). In contrast, PelI and other pectinases are secreted by the type II (Out) secretion system.

PelI has a 19-residue signal peptide that is cleaved during export. The N-terminal region of PelI (residues 20–119 as defined in the PRODOM domain database; Corpet *et al.*, 2000) exhibits a low sequence similarity to fibronectin type 3 domains, a functionally uncharacterized module present in some glycoside hydrolases and lyases (McKie *et al.*, 2001). The pectate lyase Pel-3 from *E. carotovora*, a close homologue of PelI, presents the same N-terminal extension. The role of this domain is not clear. The catalytic domain of PelI (residues 120–344) shows extensive similarity to the Pels belonging to family 3 of polysaccharide lyases and with the only known structural representative of this family, Pel-15

of *Bacillus* sp. strain KSM-P15 (Akita *et al.*, 2001). This 197-residue protein is folded into an eight-turn parallel β -helix and shows a sequence identity of 26% with PelI, suggesting that the two enzymes share the same fold. The Pel-15 active site is similar to those observed in the family 1 Pels, although the position of its divalent cation, a Ca^{2+} , does not correspond to any of the sites reported for PelC (Scavetta *et al.*, 1999).

Determination of the three-dimensional structure of the pectate lyase PelI should allow a detailed comparison of its overall fold and catalytic site with those of the other Pel families, allowing us to clarify whether these enzymes with parallel β -helix folds have evolved from a common ancestor or have arisen by convergent evolution to a closely related catalytic mechanism. Crystals of the enzyme with bound Ca^{2+} and depleted of its signal peptide have been obtained (*i.e.* PelI 20–344; MW = 35 kDa).

2. Protein expression and purification

A plasmid pTPLI (Shevchik *et al.*, 1997), used for PelI overproduction, was constructed by inserting the *Bgl*III–*Eco*RI 1.8 kbp fragment bearing the *pell* gene into pT7-6 expression vector (Tabor & Richardson, 1985). *Escherichia coli* BL21(DE3) (Stratagene) cells carrying the pTPLI plasmid were grown at 303 K in Luria broth containing $150 \mu\text{g ml}^{-1}$ ampicillin. At an OD_{600} of 1.0, isopropyl- β -D-thiogalactopyranoside (IPTG) was added to 1 mM and the cells were grown for an additional 2.5–3 h. Cells were harvested by centrifugation for 10 min at 5000g and 277 K and then frozen at 203 K. The overproduced protein was extracted from the cells by two cycles of

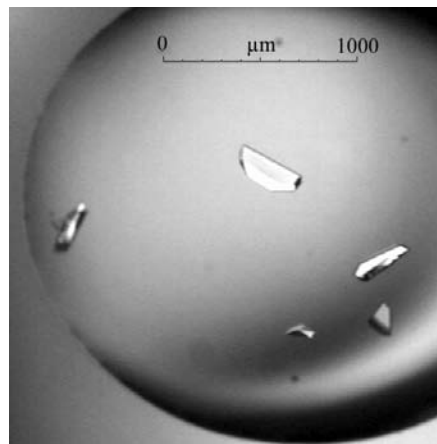


Figure 1
Crystals of PelI from *E. chrysanthemi* obtained at 292 K by the hanging-drop technique. Crystals of dimensions $0.4 \times 0.2 \times 0.1$ mm can be obtained in two weeks.

Table 1
Statistics of data processing.

	In-house native	Synchrotron native	Synchrotron derivative K Au(CN) ₂ (f''_{max})
X-ray source	Cu $K\alpha$ rotating anode	BM30A, ESRF	BM30A, ESRF
Wavelength (Å)	1.5418	0.9400	1.0400
Space group	$P2_1$	$P2_1$	$P2_1$
Unit-cell parameters (Å, °)	$a = 61.6, b = 70.7,$ $c = 73.4, \beta = 112.8$	$a = 61.6, b = 70.7,$ $c = 73.4, \beta = 112.8$	$a = 61.7, b = 70.7,$ $c = 73.5, \beta = 112.8$
Resolution range (Å)	20.0–1.6 (1.7–1.6)	20.0–1.45 (1.55–1.45)	20.0–1.6 (1.7–1.6)
Total No. of reflections	248150 (32655)	379012 (35039)	279614 (41803)
No. of unique reflections	73087 (10209)	102436 (9931)	76466 (12673)
Completeness (%)	98.3 (96.5)	99.5 (99.9)	99.7 (99.9)
Redundancy	3.4 (3.2)	3.7 (3.5)	3.7 (3.3)
$\langle I/\sigma(I) \rangle$	3.7 (2.6)	10.6 (3.4)	16.5 (6.4)
R_{sym}^\dagger (%)	9.2 (23.7)	6.5 (33.0)	4.3 (16.3)
$\sigma_{\text{norm}}/\sigma_{\text{ano}}^\ddagger$	—	1.05	1.32
Mean figure of merit (f.o.m.) §	—	—	0.33

$^\dagger R_{\text{sym}} = \sum_{hkl} \sum_i |I_i(hkl) - \langle I(hkl) \rangle| / \sum_{hkl} \sum_i I_i(hkl)$, where I_i is the i th measurement of reflection $I(hkl)$. $^\ddagger \sigma_{\text{norm}}$ and σ_{ano} are mean value of $\sigma(I)$ for acentric reflections assuming reflection $I(hkl) = I(\bar{h}\bar{k}\bar{l})$ and $I(hkl) \neq I(\bar{h}\bar{k}\bar{l})$, respectively. § f.o.m. = $|F(hkl)_{\text{best}}|/F(hkl)$, with $F(hkl)_{\text{best}} = \sum_{\alpha} P(\alpha)F_{hkl} / \sum_{\alpha} P(\alpha)$.

freeze–thawing (Johnson & Hecht, 1994) using 20 mM sodium phosphate, 5 mM EDTA pH 7. The extract was diluted with the same volume of 3.4 M ammonium sulfate, 80 mM sodium phosphate, 5 mM EDTA pH 7 and centrifuged for 20 min at 20 000g and 277 K. This sample was loaded onto a Phenyl-TSK gel (TosoHaas) column (20×2.5 cm), equilibrated with 50 mM sodium phosphate, 5 mM EDTA (buffer A) supplemented with 1.7 M $(\text{NH}_4)_2\text{SO}_4$. The column was washed with 0.2 l of the same buffer and then with 0.1 l of buffer A containing 1 M $(\text{NH}_4)_2\text{SO}_4$. The enzyme was eluted with a linear gradient of 1.0–0.5 M $(\text{NH}_4)_2\text{SO}_4$ in buffer A. The active fractions were pooled, concentrated in a Centricon 10 (Amicon) and the buffer was exchanged with 20 mM sodium acetate, 1 mM EDTA pH 5.0 (buffer B). The sample was loaded onto a Mono-Q (Pharmacia) HR 10/10 column equilibrated with buffer B and PelI was eluted with a 0–0.1 M NaCl linear gradient in buffer B. The purified enzyme was buffer-exchanged with 10 mM Tris–HCl, 0.1 mM CaCl_2 , concentrated to 10 mg ml^{-1} and stored at 253 K.

3. Crystallization

Crystallization trials were achieved using commercial screens from Hampton Research (Crystal Screens I and II, PEG, PEG-Ion and Ammonium Sulfate Screens) and Molecular Dimensions Ltd (Structure Screens I and II) using the hanging-drop vapour-diffusion technique at 277 and 292 K. The reservoirs of Limbro 24-well plates were filled with 700 μl of the crystallization solutions. Hanging drops were obtained by mixing 2 μl protein solution at 10 mg ml^{-1} with 2 μl reservoir solution. Molecular Dimensions Structure Screen II

condition No. 27 (0.01 M zinc sulfate heptahydrate, 0.1 M MES pH 6.5, 25% PEG 550) produced good crystals of dimensions up to $0.4 \times 0.2 \times 0.1$ mm within two weeks at 292 K (Fig. 1). Screening around this condition did not yield better crystals, but did show that the presence of zinc sulfate was necessary for crystallization. Crystals were mounted in a cryoloop and flash-frozen in a 100 K stream of nitrogen gas prior to data collection. X-ray measurements were taken in-house on a 345 mm MAR Research image-plate system using Cu $K\alpha$ radiation from a Nonius FR 591 rotating-anode generator equipped with Osmic mirror optics. They were cryoprotected by adding 0.5 μl ethylene glycol to the 4 μl hanging drop immediately prior to mounting (the resulting solution contains $\sim 10\%$ ethylene glycol). Crystals belong to a monoclinic space group (Table 1). The calculated V_M value is $2.1 \text{ \AA}^3 \text{ Da}^{-1}$ for two molecules in the asymmetric unit, which corresponds to a solvent content of 41% (Matthews, 1968).

4. Data collection and processing

A native data set was collected in-house to 1.6 \AA resolution. The crystal-to-detector distance was 108 mm, the oscillation step 1° and the total oscillation range 180° . Data were processed with *MOSFLM* (Leslie, 1992) and were merged, scaled and reduced with *SCALA* and *TRUNCATE* from the *CCP4* suite (Collaborative Computational Project, Number 4, 1994). Statistics are presented in Table 1. Attempts to solve the structure of PelI by the molecular-replacement method using the program *AMoRe* (Navaza, 2001) and the structure of Pel-15 (Akita *et al.*, 2001) as a model were unsuccessful. Consequently, crystals were soaked for 24–48 h in 6 μl drops of a solution of

mother liquor containing various heavy-atom salts (5–10 mM gold, mercury, lead and samarium salts) so as to solve the structure by an isomorphous replacement method. Most crystals were stable in the soaking solutions and their diffraction was tested in-house. The best derivatives were stored at 100 K in a tank of liquid nitrogen prior to synchrotron data collection at the wavelength-tunable beamline FIP-BM30A at ESRF, Grenoble, France.

5. Phasing and model building

The structure of Pell was determined using the anomalous scattering signal of a gold-derivative crystal obtained after a 48 h soak in a mother-liquor solution containing 10 mM KAu(CN)₂. The unit-cell parameters of the derivative crystal are very close to those of the native (Table 1). A fluorescence scan was taken around the gold *L*_{III} theoretical absorption edge and diffraction data were collected on a MAR CCD detector at three wavelengths corresponding to the absorption maximum ($\lambda = 1.0400 \text{ \AA}$), inflection ($\lambda = 1.0404 \text{ \AA}$) and remote ($\lambda = 0.95 \text{ \AA}$). For each wavelength, the crystal-to-detector distance was 100 mm, the oscillation step was 1° and the total oscillation range was 180° . The first data set collected at the peak with a maximum resolution of 1.6 \AA was sufficient to calculate the phases using the single anomalous dispersion method (SAD). The peak data set was processed with *XDS* and scaled with *XSCALE* (Kabsch, 1993; statistics are given in Table 1) assuming that Friedel's law was broken. A significant contribution by an anomalous scatterer to the intensities was detected by *XSCALE* with a $\sigma_{\text{norm}}/\sigma_{\text{ano}}$ value equal to 1.3 instead of 1.0 (definition in Table 1) in the resolution range 20– 1.6 \AA . A total of seven Au atoms in the asymmetric unit were detected by an automated search with the program *SOLVE* (Terwilliger & Berendzen, 1999) and phases were computed; the overall mean figure of merit (f.o.m. definition in Table 1) was 0.33. Density modification with the program *RESOLVE* (Terwilliger, 2002) resulted in an

increase in the f.o.m. to 0.52 and in an interpretable map. A model accounting for 65% of the protein was automatically built by *RESOLVE* after the last step of density modification. This model included 308 residues built according to the sequence assignment and 115 residues built without side chains. The *C α* traces of the two monomers contained in the asymmetric unit were clearly defined, as observed on a graphics station with the program *TURBO-FRODO* (Roussel & Cambillau, 1989). Subsequent attempts to include the edge and the remote data sets for phasing did not improve the quality of the electron-density maps. A rigid-body refinement of this initial structure was performed with *CNS* (Brünger *et al.*, 1998) against the in-house native data set and an *R* factor of 45% was obtained in the resolution range 15– 3 \AA . A native data set was subsequently collected at the FIP-BM30A beamline to 1.45 \AA resolution. The wavelength was 0.94 \AA , the crystal-to-detector distance 100 mm, the oscillation step 1° and the total oscillation range 180° . Data processing was performed with *XDS* (statistics in Table 1). Crystallographic refinement is in progress.

References

- Akita, M., Suzuki, A., Kobayashi, T., Ito, S. & Yamane, T. (2001). *Acta Cryst. D* **57**, 1786–1792.
- Brünger, A. T., Adams, P. D., Clore, G. M., DeLano, W. L., Gros, P., Grosse-Kunstleve, R. W., Jiang, J.-S., Kuszewski, J., Nilges, M., Pannu, N. S., Read, R. J., Rice, L. M., Simonson, T. & Warren, G. L. (1998). *Acta Cryst. D* **54**, 905–921.
- Buttner, D. & Bonas, U. (2003). *Curr. Opin. Plant Biol.* **6**, 312–319.
- Charnock, S. J., Brown, I. E., Turkenburg, J. P., Black, G. W. & Davies, G. J. (2002). *Proc. Natl Acad. Sci. USA*, **99**, 12067–12072.
- Collaborative Computational Project, Number 4 (1994). *Acta Cryst. D* **50**, 760–763.
- Corpet, F., Servant, F., Gouzy, J. & Kahn, D. (2000). *Nucleic Acids Res.* **28**, 267–269.
- Coutinho, P. M. & Henrissat, B. (1999). *Recent Advances in Carbohydrate Bioengineering*, edited by H. J. Gilbert, G. Davies, B. Henrissat & B. Svensson, pp. 3–12. Cambridge: The Royal Society of Chemistry.
- Gaudriault, S., Brisset, M. N. & Barny, M. A. (1998). *FEBS Lett.* **428**, 224–228.

- Herron, S. R., Scavetta, R. D., Garrett, M., Legner, M. & Journak, F. (2003). *J. Biol. Chem.* **278**, 12271–12277.
- Jenkins, J., Mayans, O., Smith, D., Worboys, K. & Pickersgill, R. (2001). *J. Mol. Biol.* **305**, 951–960.
- Johnson, B. H. & Hecht, M. H. (1994). *Biotechnology (NY)*, **12**, 1357–1360.
- Journak, F., Yoder, M. D., Pickersgill, R. & Jenkins, J. (1994). *Curr. Opin. Struct. Biol.* **4**, 802–806.
- Kabsch, W. (1993). *J. Appl. Cryst.* **26**, 795–800.
- Leitzke, S. E., Yoder, M. D., Keen, N. T. & Journak, F. (1994). *Plant Physiol.* **106**, 849–862.
- Leslie, A. G. W. (1992). *Jnt CCP4/ESF-EACBM Newsl. Protein Crystallogr.* **26**.
- McKie, V. A., Vincken, J. P., Voragen, A. G., van den Broek, L. A., Stimson, E. & Gilbert, H. J. (2001). *Biochem. J.* **355**, 167–177.
- Matthews, B. W. (1968). *J. Mol. Biol.* **33**, 491–497.
- Mayans, O., Scott, M., Connerton, I., Gravesen, T., Benen, J., Visser, J., Pickersgill, R. & Jenkins, J. (1997). *Structure*, **5**, 677–689.
- Navaza, J. (2001). *Acta Cryst. D* **57**, 1367–1372.
- Petersen, T. N., Kauppinen, S. & Larsen, S. (1997). *Structure*, **5**, 533–544.
- Pickersgill, R., Jenkins, J., Harris, G., Nasser, W. & Robert-Baudouy, J. (1994). *Nature Struct. Biol.* **1**, 717–723.
- Pickersgill, R., Smith, D., Worboys, K. & Jenkins, J. (1998). *J. Biol. Chem.* **273**, 24660–24664.
- Robert-Baudouy, J., Nasser, W., Condemine, G., Reverchon, S., Shevchik, V. E. & Hugouvieux-Cotte-Pattat, N. (2000). *Plant-Microbe Interactions*, edited by G. Stacey & N. T. Keen, pp. 221–268. St Paul, USA: APS Press.
- Roussel, A. & Cambillau, C. (1989). *Silicon Graphics Geometry Partners Directory*, edited by Silicon Graphics, pp. 77–78. Mountain View, CA, USA: Silicon Graphics.
- Scavetta, R. D., Herron, S. R., Hotchkiss, A. T., Kita, N., Keen, N. T., Benen, J. A., Kester, H. C., Visser, J. & Journak, F. (1999). *Plant Cell*, **11**, 1081–1092.
- Shevchik, V. E., Boccara, M., Vedel, R. & Hugouvieux-Cotte-Pattat, N. (1998). *Mol. Microbiol.* **29**, 1459–1469.
- Shevchik, V. E., Condemine, G., Robert-Baudouy, J. & Hugouvieux-Cotte-Pattat, N. (1999). *J. Bacteriol.* **181**, 3912–3919.
- Shevchik, V. E., Robert-Baudouy, J. & Hugouvieux-Cotte-Pattat, N. (1997). *J. Bacteriol.* **179**, 7321–7330.
- Tabor, S. & Richardson, C. C. (1985). *Proc. Natl Acad. Sci. USA*, **82**, 1074–1078.
- Terwilliger, T. C. (2002). *Acta Cryst. D* **58**, 1937–1940.
- Terwilliger, T. C. & Berendzen, J. (1999). *Acta Cryst. D* **55**, 849–861.
- Thomas, L. M., Doan, C. N., Oliver, R. L. & Yoder, M. D. (2002). *Acta Cryst. D* **58**, 1008–1015.
- Vitali, J., Schick, B., Kester, H. C., Visser, J. & Journak, F. (1998). *Plant Physiol.* **116**, 69–80.
- Yoder, M. D., Lietzke, S. E. & Journak, F. (1993). *Structure*, **1**, 241–251.